ELEKTRYKA 2011
Zeszyt 4 (220) Rok LVII

Paweł JABŁOŃSKI
Electrical Engineering Faculty, Częstochowa University of Technology

APPROXIMATE BEM ANALYSIS OF THIN ELECTROMAGNETIC SHIELD

Summary. A method of approximate analysis of a thin electromagnetic shield is considered and proposed in the paper. Due to presumably small thickness of the shield, its numerical analysis is troublesome. Applying the Boundary Element Method (BEM) to solve equations for a thin shield creates two difficulties: significant increase of the number of algebraic equations, and the presence of nearly singular integrals. The proposed model avoids them both by using an approximate analytical solution for the shield. Numerical examples confirm its usability.

Keywords: BEM, thin shells, electromagnetic shielding, Helmholtz equation

PRZYBLIŻONA ANALIZA CIENKOŚCIENNEGO EKRANU ELEKTROMAGNETYCZNEGO Z UŻYCIEM MEB

Streszczenie. W pracy zaproponowano przybliżoną metodę analizy pola elektromagnetycznego w otoczeniu cienkościennego ekranu elektromagnetycznego z zastosowaniem metody elementów brzegowych (MEB). Z powodu założonej niewielkiej grubości ekranu analiza numeryczna napotyka na problemy. Zastosowanie MEB niesie ze sobą dwie trudności: znaczny wzrost liczby równań algebraicznych oraz obecność całek prawieosobliwych. Przedstawiona metoda unika obydwu trudności poprzez zastosowanie przybliżonego analitycznego rozwiązania w obszarze ekranu. Zaprezentowane przykłady numeryczne potwierdzają jej użyteczność w rozpatrywanej klasie zagadnień.

Słowa kluczowe: MEB, cienkie powłoki, ekranowanie elektromagnetyczne, równanie Helmholtza

1. INTRODUCTION

Some sort of equipment needs electromagnetic (EM) shielding, which can be achieved by placing it in a conductive shell (enclosure). Analysis of EM field in such a configuration requires solving the field equations at least in three regions. Besides, geometrical complexity of the problem involves numerical methods. One of such methods can be BEM (boundary element method) [1, 2, 6, 10, 13], especially, if the exterior extends considerably. However, if

the shield is relatively thin, the problem of suitable discretization of its surface appears. In addition, some BEM integrals become nearly singular, what requires specific treatment and enlarges the overall computational effort. For that reason, such thin shells should be treated in a special way. For example, thin shells have been considered in [3-5, 7-11], to recall a few only. This paper presents an approximate method of reducing the BEM equations arising in EM shielding analysis. For simplicity, the considerations are limited to 2D problems.

2. PROBLEM DESCRIPTION AND BEM ANALYSIS

2.1. Problem description and governing equations

An EM shield, Ω_1, is placed in free space, Ω_0, and encloses the protected region, Ω_2 – Fig. 1. The external and internal surfaces of the shield are referred to as S_1 and S_2, respectively. The shield is considered to be very thin of constant thickness d, relative permeability μ_{r1} = const, and electric conductivity γ_1 = const, while $\mu = \mu_0$ and $\gamma = 0$ in the protected region and the free space. Such a configuration is affected by an external transverse harmonic magnetic field, $\boldsymbol{B}_s$, of angular frequency ω.

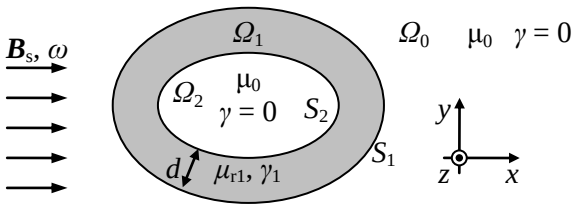

Fig. 1. Problem description
Rys. 1. Konfiguracja obliczeniowa

In 2D problems the vector magnetic potential $\boldsymbol{A}$ ($\boldsymbol{B} = \nabla\times\boldsymbol{A}$) can be chosen to have only a z-component. Time harmonic dependency of excitation $\boldsymbol{B}_s$ permits using the phasor notation. The phasor of the z-component of vector magnetic potential $\boldsymbol{A}$ fulfills the following equations in particular regions [12, 14]:

$$\begin{cases} \nabla^2 \underline{A}^{(m)} = 0 & \text{for } \Omega_m,\ m = 0, 2, \\ \nabla^2 \underline{A}^{(1)} - \kappa^2 \underline{A}^{(1)} = 0 & \text{for } \Omega_1. \end{cases} \tag{1}$$

where

$$\kappa^2 = \mathrm{j}\omega\mu_{r1}\mu_0\gamma_1, \tag{2}$$

and j is the imaginary unit. Field continuity conditions on boundaries S_1 and S_2 are as follows:

$$\underline{A}^{(0)}\Big|_{S_1} = \underline{A}^{(1)}\Big|_{S_1}, \qquad \underline{A}^{(1)}\Big|_{S_2} = \underline{A}^{(2)}\Big|_{S_2}, \tag{3}$$

$$\frac{\partial \underline{A}^{(0)}}{\partial n}\Big|_{S_1} = -\frac{1}{\mu_{\mathrm{r}1}}\frac{\partial \underline{A}^{(1)}}{\partial n}\Big|_{S_1}, \qquad \frac{\partial \underline{A}^{(2)}}{\partial n}\Big|_{S_2} = -\frac{1}{\mu_{\mathrm{r}1}}\frac{\partial \underline{A}^{(1)}}{\partial n}\Big|_{S_2}, \tag{4}$$

Far from the shield, theoretically − in the infinity, where the influence of the shield, the vector magnetic potential tends to the vector magnetic potential of externally applied magnetic field:

$$\underline{A}\big|_{\infty} \to \underline{A}_{\mathrm{s}}, \tag{5}$$

where $\underline{A}_s$ is chosen so that

$$\underline{\boldsymbol{B}}_{\mathrm{s}} = \nabla \times (\underline{A}_{\mathrm{s}} \boldsymbol{1}_z). \tag{6}$$

2.2. Standard BEM model

The standard BEM applied to this problem leads to the following system of equations:

$$\left.\begin{aligned} &\mathbf{H}_1^{(0)}\mathbf{A}_1^{(0)} = \mathbf{G}_1^{(0)}\mathbf{Q}_1^{(0)} + \mathbf{A}_{\mathrm{s}} \\ &\mathbf{H}_1^{(1)}\mathbf{A}_1^{(1)} + \mathbf{H}_2^{(1)}\mathbf{A}_2^{(1)} = \mathbf{G}_1^{(1)}\mathbf{Q}_1^{(1)} + \mathbf{G}_2^{(1)}\mathbf{Q}_2^{(1)} \\ &\mathbf{H}_2^{(2)}\mathbf{A}_2^{(2)} = \mathbf{G}_2^{(2)}\mathbf{Q}_2^{(2)} \end{aligned}\right\}. \tag{7}$$

Vectors $\mathbf{A}_l^{(m)}$ and $\mathbf{Q}_l^{(m)}$ contain nodal values of $\underline{A}^{(m)}$ and $\partial_n \underline{A}^{(m)}$ on boundary S_l. Vector $\mathbf{A}_{\mathrm{s}}$ contain nodal values of potential $\underline{A}_{\mathrm{s}}$ on boundary S_1. Matrices $\mathbf{G}_l^{(m)}$ and $\mathbf{H}_l^{(m)}$ are built from boundary integrals $g_{ijk}^{(m)}$ and $h_{ijk}^{(m)}$, respectively, where

$$g_{ijk}^{(m)} = \int_{S_j} N_k G^{(m)}\,\mathrm{d}S, \qquad h_{ijk}^{(m)} = \int_{S_j} N_k \frac{\partial G^{(m)}}{\partial n}\,\mathrm{d}S, \tag{8}$$

where N_k are shape functions used for approximation of $\underline{A}$ and $\partial_n \underline{A}$ in boundary elements, and $G^{(m)}$ is the fundamental solution of equation for domain Ω_m. The fundamental solution depends on the distance, R, between arbitrary point i and point P lying on boundary S. It equals

$$G(R) = \frac{1}{2\pi}\ln\frac{1}{R} \tag{9}$$

for $\kappa = 0$ (domains Ω_0 and Ω_2), and

$$G(R) = \frac{1}{2\pi} K_0(\kappa R) \tag{10}$$

for $\kappa \neq 0$ (domain Ω_1), where K_0 is the modified Bessel function of the second kind of order 0. Detailed construction of matrices $\mathbf{G}_l^{(m)}$ and $\mathbf{H}_l^{(m)}$ is presented in [2, 6, 10].

Boundary conditions (3) and (4) rewritten in discrete form are as follows:

$$\mathbf{A}_1^{(0)} = \mathbf{A}_1^{(1)} = \mathbf{A}_1, \qquad \mathbf{A}_2^{(1)} = \mathbf{A}_2^{(2)} = \mathbf{A}_2, \tag{11}$$

$$\mathbf{Q}_1^{(0)} = -\beta \mathbf{Q}_1^{(1)}, \qquad \mathbf{Q}_2^{(2)} = -\beta \mathbf{Q}_2^{(1)}, \tag{12}$$

where

$$\beta = \frac{1}{\mu_{\mathrm{r}1}}. \tag{13}$$

The final equations can be written as

$$\begin{bmatrix} \mathbf{H}_1^{(0)} & \beta\mathbf{G}_1^{(0)} & \mathbf{0} & \mathbf{0} \\ \mathbf{H}_1^{(1)} & -\mathbf{G}_1^{(1)} & \mathbf{H}_2^{(1)} & -\mathbf{G}_2^{(1)} \\ \mathbf{0} & \mathbf{0} & \mathbf{H}_2^{(2)} & \beta\mathbf{G}_2^{(2)} \end{bmatrix} \begin{Bmatrix} \mathbf{A}_1 \\ \mathbf{Q}_1^{(1)} \\ \mathbf{A}_2 \\ \mathbf{Q}_2^{(1)} \end{Bmatrix} = \begin{Bmatrix} \mathbf{A}_{\mathrm{s}} \\ \mathbf{0} \\ \mathbf{0} \end{Bmatrix}. \tag{14}$$

The system of equations, from now on referred to as the *standard BEM model*, is mathematically correct for any values of parameters (such as d, β, $\underline{A}_{\mathrm{s}}$, boundary shapes). However, numerical tests show that small values of d can be troublesome. This is because the integrands in integrals (8) can have very sharp peaks (but still finite). Such integrals are called nearly singular, by analogy to singular integrals, whose integrands have infinite peaks. Numerical evaluation of nearly singular integrals require a considerable computational effort, and even then can lead to significant numerical errors. Moreover, since corresponding nodes on S_1 and S_2 become very close, the BEM equations for them are almost linearly dependent. These two disadvantages lead to troubles during numerical computations.

2.3. Approximate BEM model

There are some methods of avoiding the aforementioned disadvantages [3-5, 7-11]. The one presented here consist in using a semi-analytical solution in the thin shield. The first idea that comes on mind is similar to presented in [3, 5], and consists in expanding the solution in the shell into power series. As a result, the values of $\underline{A}$ and $\partial_n \underline{A}$ at the corresponding points lying on boundaries S_1 and S_2 are connected with the following approximate relationship:

$$\underline{Q}_1^{(1)} = \left.\frac{\partial \underline{A}_1}{\partial n}\right|_{S_1} \approx \frac{\underline{A}_1 - \underline{A}_2}{d}. \tag{15}$$

Unfortunately, this implies $\underline{Q}_2^{(1)} = -\underline{Q}_1^{(1)}$, and no information on value of κ can be introduced into the equations. Therefore, this approach must be rejected, and a method of taking into account κ must be found.

To achieve this, observe that if the shield is thin enough and the BEM discretization is fine enough, the shell between two corresponding boundary elements lying on S_1 and S_2 may be approximately regarded as a fragment of infinite plate. In such a plate the general solution of the second of Eqs. (1) for $\kappa \neq 0$ can be expressed as

$$\underline{A}(x) = C_1 \cosh \kappa x + C_2 \sinh \kappa x, \tag{16}$$

where C_1 and C_2 are constants. Assuming that $\underline{A}(0) = \underline{A}_1$ and $\underline{A}(d) = \underline{A}_2$, one can eliminate the constants and obtain

$$\underline{A}(x) = \frac{\underline{A}_1 \sinh \kappa(d-x) + \underline{A}_2 \sinh \kappa x}{\sinh \kappa d}, \tag{17}$$

and consequently,

$$\frac{\partial \underline{A}}{\partial x} = \kappa \frac{-\underline{A}_1 \cosh \kappa(d-x) + \underline{A}_2 \cosh \kappa x}{\sinh \kappa d}. \tag{18}$$

Therefore, the normal derivatives of $\underline{A}$ for $x = 0$ and d, can be expressed as

$$\underline{Q}_1 = -\left.\frac{\partial \underline{A}}{\partial x}\right|_0 = \sigma \underline{A}_1 - \tau \underline{A}_2, \tag{19}$$

$$\underline{Q}_2 = \left.\frac{\partial \underline{A}}{\partial x}\right|_d = -\tau \underline{A}_1 + \sigma \underline{A}_2, \tag{20}$$

where

$$\sigma = \frac{\kappa \cosh \kappa d}{\sinh \kappa d}, \qquad \tau = \frac{\kappa}{\sinh \kappa d}. \tag{21}$$

Applying Eqs. (19) and (20) to the thin shield yields the following approximate relationships:

$$\mathbf{Q}_1^{(1)} \approx \sigma \mathbf{A}_1 - \tau \mathbf{A}_2, \qquad \mathbf{Q}_2^{(1)} \approx -\tau \mathbf{A}_1 + \sigma \mathbf{A}_2. \tag{22}$$

It is worth noting that the approach described in [3, 5] can be obtained exactly in the same way. In fact, Eqs. (21) for $\kappa \to 0$ give

$$\lim_{\kappa\to 0}\sigma=\lim_{\kappa\to 0}\tau=\frac{1}{d}, \tag{23}$$

and relationship (19) becomes identical with (15).

Using Eqs. (22) in (14) allows eliminating the BEM equations for the shield. The resulting equations are as follows

$$\begin{bmatrix}\mathbf{H}_1^{(0)}+\sigma\beta\mathbf{G}_1^{(0)} & -\tau\beta\mathbf{G}_1^{(0)}\\ -\tau\beta\mathbf{G}_2^{(2)} & \mathbf{H}_2^{(2)}+\sigma\beta\mathbf{G}_2^{(2)}\end{bmatrix}\begin{Bmatrix}\mathbf{A}_1\\ \mathbf{A}_2\end{Bmatrix}=\begin{Bmatrix}\mathbf{A}_\mathrm{s}\\ \mathbf{0}\end{Bmatrix}. \tag{24}$$

In the subsequent paragraphs, the system of equations is called the *approximate BEM model* (ABEM). It has half the number of equations given by the standard BEM model (14) and no nearly singular integrals occur in it (for sufficiently regular boundary). However, one should keep in mind that this model is a result of assumption that the shell can be locally treated as planar. In fact, this not always may be acceptable, but there are situations in which it should work well.

3. NUMERICAL RESULTS

3.1. General remarks

Both models were implemented in Mathematica 7.0 and tested in various conditions. The considered shields were long cylinders of very thin walls and constant cross-section. It was assumed that the externally applied magnetic field $\boldsymbol{B}_\mathrm{s}$ was uniform and had the following form

$$\underline{\boldsymbol{B}}_\mathrm{s}=B_0\boldsymbol{1}_x,\qquad \underline{A}_\mathrm{s}=\underline{B}_0 y\,. \tag{25}$$

Two kinds of boundary elements were used in numerical tests: constant (with one node in the midpoint) and quadratic (with three nodes in the beginning, midpoint and endpoint). This refers, however, only to the field approximation ($\underline{A}$ and $\partial_n\underline{A}$), since the geometry was always approximated with quadratic curves. This allowed taking into account the shape of boundary quite precisely. The same set of nodes was used for both kinds of elements.

Equation systems (14) and (24) were solved with use of Mathematica's built-in routines (`LinearSolve`). Integrals (8) were evaluated as follows:

- for Laplace equation (domains Ω_0 and Ω_2): analytical integration for straight geometry, special treatment with use of logarithmic Gaussian quadrature for singular cases and curvilinear geometry, numerical integration according to the four-zoned scheme described thoroughly in [3],

- for Helmholtz equation (domain Ω_1, only the standard BEM): special treatment with singularity exclusion for singular cases, numerical integration based on the four-zoned scheme for non-singular cases.

The four-zoned scheme introduces four zones, whose limits are determined by the endpoints of a boundary element and three parameters $0 < s_1 < s_2 < s_3 < \infty$. Depending on the zone in which point i is located, different integration method or quadrature order is used, in accordance to the rule: "the closer the point to the boundary element the more refined integration". In the nearest zone, the Mathematica's built-in function (`NIntegrate`) is used to gain appropriate accuracy with minimal programming effort, and in the other zones – the Gaussian quadrature of orders $GQO_1 > GQO_2 > GQO_3 > 0$ (to decrease computation time). Plots show the actual values of the integration parameters as "$>s_1$:GQO_1>s_2:GQO_2>s_3:GQO_3".

3.2. Cylindrical shield

The first benchmark problem was a cylindrical shield of circular cross-section (Fig. 2), whose internal and external radii were R_2 and $R_1 = R_2 + d$, respectively. It was used to check the validity of both models, because it has an analytical solution, which is as follows:

$$\underline{A}^{(0)} = B_0 R_1 \left(1 + \frac{v - w}{v + w} \frac{R_1^2}{r^2} \right) \frac{r}{R_1} \sin\varphi \,, \tag{26}$$

$$\underline{A}^{(1)} = B_0 R_1 \frac{2}{v + w} [\, p I_1(\kappa r) - q K_1(\kappa r)] \sin\varphi \,, \tag{27}$$

$$\underline{A}^{(2)} = B_0 R_1 \frac{2\beta(1+\delta)}{v + w} \frac{r}{R_1} \sin\varphi \,, \tag{28}$$

where $I_1(z)$ and $K_1(z)$ are modified Bessel functions of the first and second kind of order one, respectively, β is given by Eq. (13), δ is the relative thickness of the shell defined as

$$\delta = \frac{d}{R_2} \,, \tag{29}$$

and

$$p = K_1(\kappa R_2) - \beta \kappa R_2 K_1'(\kappa R_2) \,, \tag{30}$$

$$q = I_1(\kappa R_2) - \beta \kappa R_2 I_1'(\kappa R_2) \,, \tag{31}$$

$$v = p I_1(\kappa R_1) - q K_1(\kappa R_1) \,, \tag{32}$$

$$w = \beta \kappa R_1 [\, p I_1'(\kappa R_1) - q K_1'(\kappa R_1)] \,. \tag{33}$$

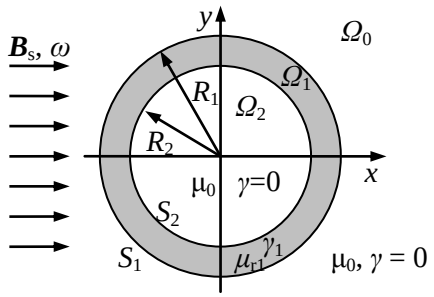

Fig. 2. Cylindrical EM shield in a transverse uniform time harmonic external magnetic field
Rys. 2. Cylindryczny ekran EM w poprzecznym równomiernym harmonicznym polu magnetycznym

The approximate BEM model uses relationships (22). It is worth to investigate if they are applicable for cylindrical shield. To find it out it is necessary to evaluate the equivalents of coefficients σ and τ and compare them with expressions (21). From Eqs. (26) and (28) through continuity conditions (3) one obtains, respectively

$$\underline{A}_1 = \underline{A}^{(0)}\Big|_{r=R_1} = B_0 R_1 \frac{2\nu}{\nu + w}\sin\varphi,$$

$$\underline{A}_2 = \underline{A}^{(2)}\Big|_{r=R_2} = B_0 R_1 \frac{2\beta}{\nu + w}\sin\varphi.$$

The same equations with continuity conditions (4) lead to expressions for the normal derivatives on S_1 and S_2:

$$\underline{Q}_1^{(1)} = \frac{\partial \underline{A}^{(1)}}{\partial r}\bigg|_{r=R_1} = \frac{1}{\beta}\frac{\partial \underline{A}^{(0)}}{\partial r}\bigg|_{r=R_1} = B_0 \frac{1}{\beta}\frac{2w}{\nu + w}\sin\varphi,$$

$$\underline{Q}_2^{(1)} = -\frac{\partial \underline{A}^{(1)}}{\partial r}\bigg|_{r=R_2} = -\frac{1}{\beta}\frac{\partial \underline{A}^{(2)}}{\partial r}\bigg|_{r=R_2} = -B_0 \frac{2(1+\delta)}{\nu + w}\sin\varphi.$$

By requiring to satisfy the following relationships:

$$\begin{cases} \underline{Q}_1^{(1)} = \sigma' \underline{A}_1 - \tau' \underline{A}_2, \\ \underline{Q}_2^{(1)} = -\tau' \underline{A}_1 + \sigma' \underline{A}_2, \end{cases}$$

one finds that

$$\sigma' = \frac{1}{\beta R_1}\frac{w\nu + (1+\delta)\beta^2}{\nu^2 - \beta^2}, \qquad \tau' = \frac{1}{R_1}\frac{\nu(1+\delta) + w}{\nu^2 - \beta^2}. \tag{34}$$

These expressions for small δ should be compared with those given by Eqs. (21). It is convenient to introduce the dimensionless parameter $\mathcal{K}$ defined as

$$\mathcal{K} = \kappa R_2 = k + \mathrm{j}k\,. \tag{35}$$

Since $\kappa R_1 = \kappa R_2(1 + \delta) = \mathcal{K} + \mathcal{K}\delta$, quantities (30)-(33), and consequently (34), can be expressed in terms of dimensionless parameters $\mathcal{K}$, δ and β. The goal is to consider their approximate values for small δ. This is considered separately for $|\mathcal{K}\delta| << 1$ and $|\mathcal{K}\delta| \geq O(1)$. If Δ is the skin depth for the shield, it holds

$$\mathcal{K}\delta = \kappa d = \frac{d}{\Delta}(1 + \mathrm{j})\,. \tag{36}$$

Thus, case $|\mathcal{K}\delta| << 1$ is equivalent to $d << \Delta$, what corresponds to a small attenuation in the shield, while $|\mathcal{K}\delta| \geq O(1)$ is equivalent to $d \geq O(\Delta)$ – a relatively large attenuation.

Beginning with the last case, observe that it implies $|\mathcal{K}| >> 1$ (since $\delta << 1$). Therefore, using the following asymptotic expansions for $|z| >> 1$:

$$I_1(z) \approx I_1'(z) \approx \frac{1}{\sqrt{2\pi z}}\mathrm{e}^{z}, \qquad K_1(z) \approx -K_1'(z) \approx \sqrt{\frac{\pi}{2z}}\mathrm{e}^{-z}, \tag{37}$$

it is easy to show that

$$v \approx \frac{\sinh\mathcal{K}\delta + \beta\mathcal{K}\cosh\mathcal{K}\delta}{\mathcal{K}}, \qquad w \approx \beta(\cosh\mathcal{K}\delta + \beta\mathcal{K}\sinh\mathcal{K}\delta),$$

and consequently, after some transformations

$$\sigma' \approx \kappa\frac{\cosh\kappa d}{\sinh\kappa d} = \sigma, \qquad \tau' \approx \kappa\frac{1}{\sinh\kappa d} = \tau\,. \tag{38}$$

It is worth noting that β does not matter at all in this case.

If $|\mathcal{K}\delta| << 1$, we can use expansions into power series of $\mathcal{K}\delta$. Using various identities for Bessel functions, like

$$I_\nu'(z)K_\nu(z) - I_\nu(z)K_\nu'(z) = \frac{1}{z},$$

or just Mathematica's function `Series`, it can be shown that up to linear terms in $\mathcal{K}\delta$, u and v are

$$v \approx \beta + \delta, \qquad w \approx \beta + (1+\mathcal{K}^2)\beta^2\delta\,,$$

yielding

$$\sigma' \approx \frac{1}{d}\frac{[1+(1+\mathcal{K}^2)\beta\delta]\delta + [2+(1+\mathcal{K}^2)\beta\delta]\beta}{\delta + 2\beta}, \qquad \tau' \approx \frac{1}{d}\frac{\delta + [2+(1+\mathcal{K}^2)\beta\delta]\beta}{\delta + 2\beta}. \tag{39}$$

As long as

$$\left|1+\mathcal{K}^2\right|\beta\delta << 1, \tag{40}$$

both σ' and τ' simplify to $1/d$, just as σ and τ (see Eq. (23)). Certainly, this holds for sufficiently small $\beta\delta$ (i.e. $\mu_{r1} >> \delta$), what includes both magnetic and non-magnetic shields in static as well as low-frequency magnetic fields. Concluding, Eqs. (21)-(22), and consequently, the approximate BEM model (24), should work properly for any values of $|\mathcal{K}|$. Although the considerations concern a cylindrical shield, it seems to be in force also for shields of other shapes. This is confirmed in the subsequent numerical simulations.

Both models, the standard and approximate, were tested for various values of parameters δ, $\mathcal{K}$ and β, with quadratic or constant boundary elements. Results of numerical computations for exemplary values of parameters are shown in plots of boundary values of $\underline{A}$ and $\underline{B}_t = -\partial_n \underline{A}^{(1)}$ (with normal direction outwards the shield). Values of $\underline{A}$ are given in units of $B_0 R_1$, values of $\underline{B}_t$ in units of B_0 and the horizontal axis identifies the index of boundary node. In some cases, plots of errors of potential ($\delta\underline{A}$) and tangential component of magnetic field intensity ($\delta\underline{B}_t$) in particular boundary nodes are more informative. The errors are defined as follows:

$$\delta\underline{A} = \frac{\underline{A}_{\mathrm{num}} - \underline{A}_{\mathrm{th}}}{\left|\underline{A}_{\mathrm{th}}\right|_{\max}} \cdot 100\%, \tag{41}$$

$$\delta\underline{B}_t = \frac{\underline{B}_{t\mathrm{num}} - \underline{B}_{t\mathrm{th}}}{\left|\underline{B}_{t\mathrm{th}}\right|_{\max}} \cdot 100\%, \tag{42}$$

where “th” and “num” refer to the theoretical value and its numerical estimate, respectively. Quantities $|\underline{A}_{\mathrm{th}}|_{\max}$ and $|B_{t\mathrm{th}}|_{\max}$ are the maximal values of $|\underline{A}_{\mathrm{th}}|$ and $|\underline{B}_{t\mathrm{th}}|$ on boundary S_1 or S_2.

Figure 3 shows values of $|\underline{A}|$ and $|\underline{B}_t|$ for δ = 0.1, $\mathcal{K}$ = 10, μ_{r1} = 1 and 1000, and constant boundary elements (for quadratic elements the results are very similar). This cases correspond to a relatively thick non-ferromagnetic or ferromagnetic EM shield. The approximate model gives quite accurate results, although the standard BEM is more accurate in this case (due to large enough δ).

Figure 4 show values of $|\delta\underline{A}|$ and $|\delta\underline{B}_t|$ for δ = 0.01, $\mathcal{K}$ = 10, μ_{r1} = 1 or 1000 for constant boundary elements, and Figure 5 – for quadratic elements. In both cases, the approximate BEM model gives errors comparable with the standard BEM model, and they usually are below 1%. Surprisingly, quadratic elements give unpleasant oscillations in boundary values, and errors $|\delta\underline{B}_t|$ are larger for the standard BEM.

Figure 6 show values of errors $|\delta\underline{A}|$ and $|\delta\underline{B}_t|$ for the same parameters, except for $\mathcal{K}$ = 100, and constant elements. This time the approximate model gives more accurate results, with errors below 1%, whereas the standard BEM leads to considerable errors.

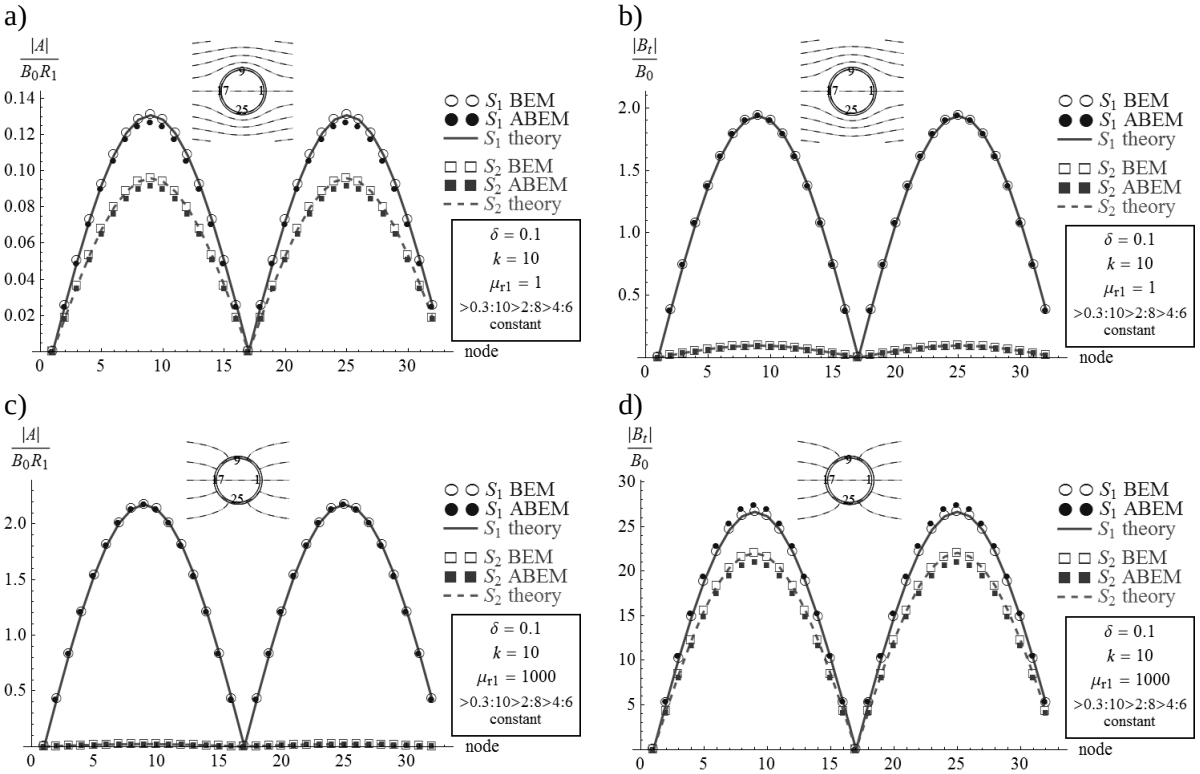

Fig. 3. Magnitudes of potential $\underline{A}$ (a, c) and tangential component of magnetic flux density $\underline{B}_t$ (b, d) on boundaries S_1 and S_2 for $\delta = 0.1$, $k = 10$ with $\mu_{r1} = 1$ (a, b) or $\mu_{r1} = 1000$ (c, d)

Rys. 3. Magnitudy potencjału $\underline{A}$ (a, c) i składowej stycznej indukcji magnetycznej $\underline{B}_t$ (b, d) na brzegach S_1 i S_2 dla $\delta = 0.1$, $k = 10$ oraz $\mu_{r1} = 1$ (a, b) i $\mu_{r1} = 1000$ (c, d)

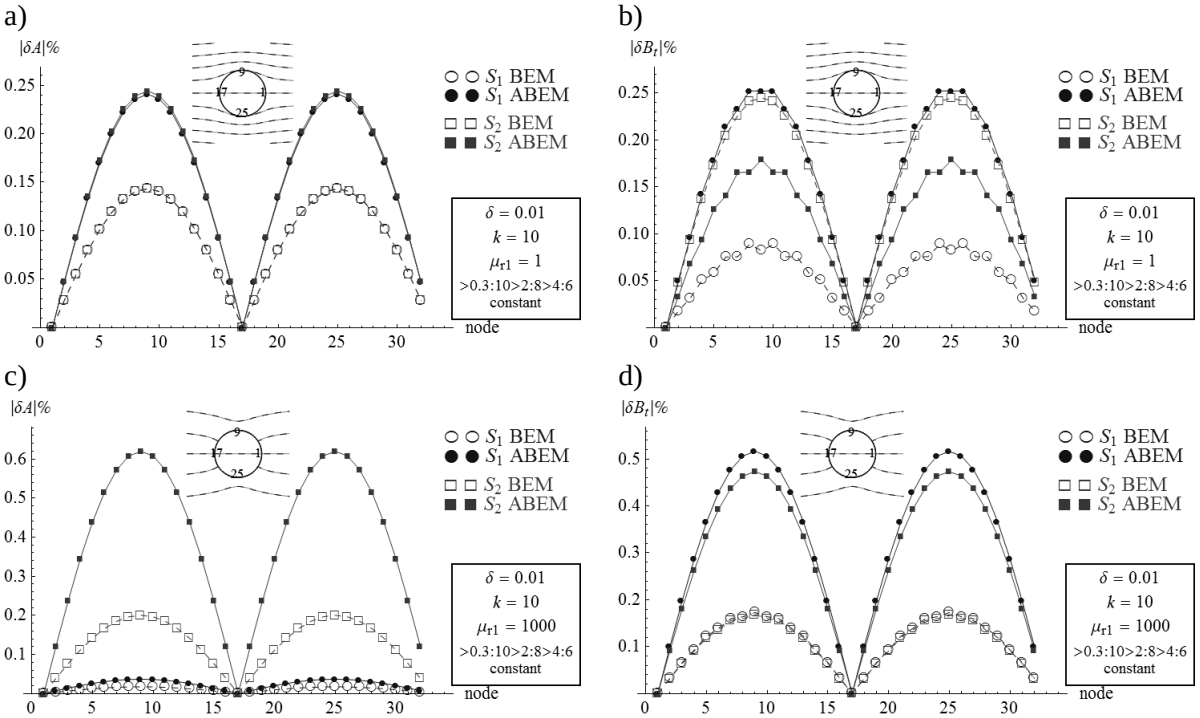

Fig. 4. Magnitudes of errors $\delta\underline{A}$ (a, c) and $\delta\underline{B}_t$ (b, d) on boundaries S_1 and S_2 for $\delta = 0.01$, $k = 10$ with $\mu_{r1} = 1$ (a, b) or $\mu_{r1} = 1000$ (c, d) for 32 constant elements

Rys. 4. Magnitudy błędów $\delta\underline{A}$ (a, c) i $\delta\underline{B}_t$ (b, d) na brzegach S_1 i S_2 dla $\delta = 0.01$, $k = 10$ oraz $\mu_{r1} = 1$ (a, b) i $\mu_{r1} = 1000$ (c, d) dla 32 elementów stałych

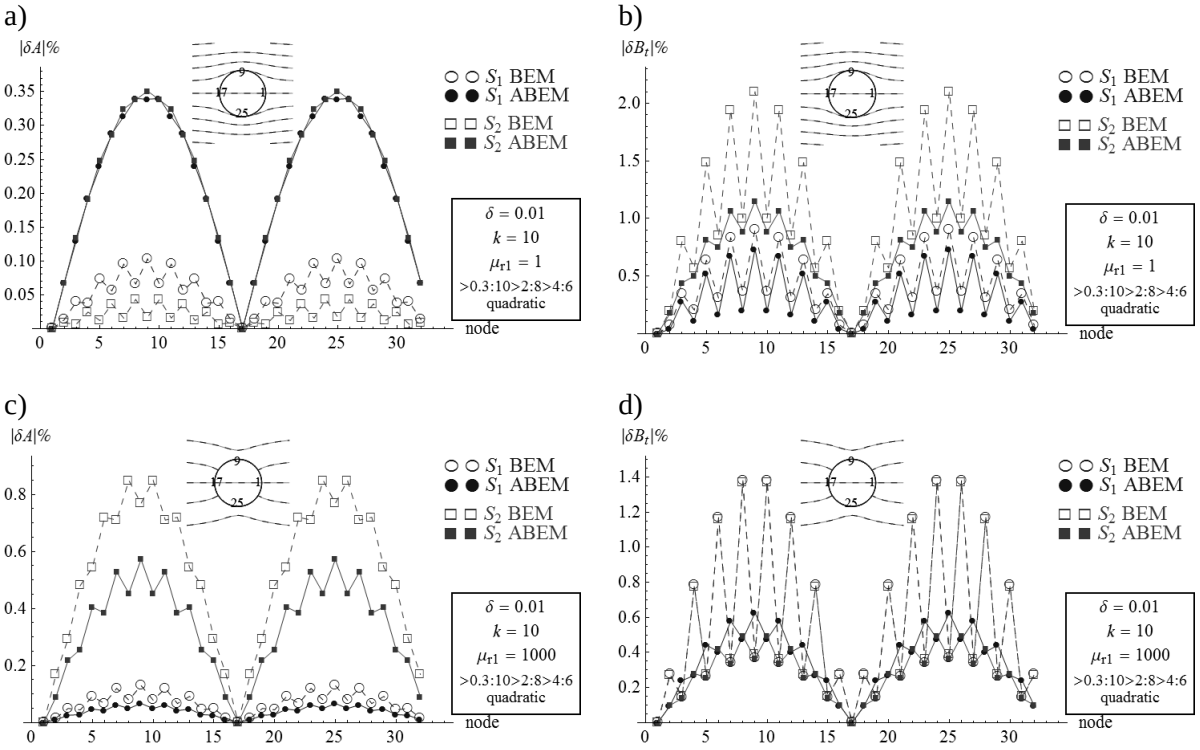

Fig. 5. Magnitudes of errors $\delta\underline{A}$ (a, c) and $\delta\underline{B}_t$ (b, d) on boundaries S_1 and S_2 for $\delta = 0.01$, $k = 10$ with $\mu_{r1} = 1$ (a, b) or $\mu_{r1} = 1000$ (c, d) for 16 quadratic elements

Rys. 5. Magnitudy błędów $\delta\underline{A}$ (a, c) i $\delta\underline{B}_t$ (b, d) na brzegach S_1 i S_2 dla $\delta = 0.01$, $k = 10$ oraz $\mu_{r1} = 1$ (a, b) i $\mu_{r1} = 1000$ (c, d) dla 16 elementów kwadratowych

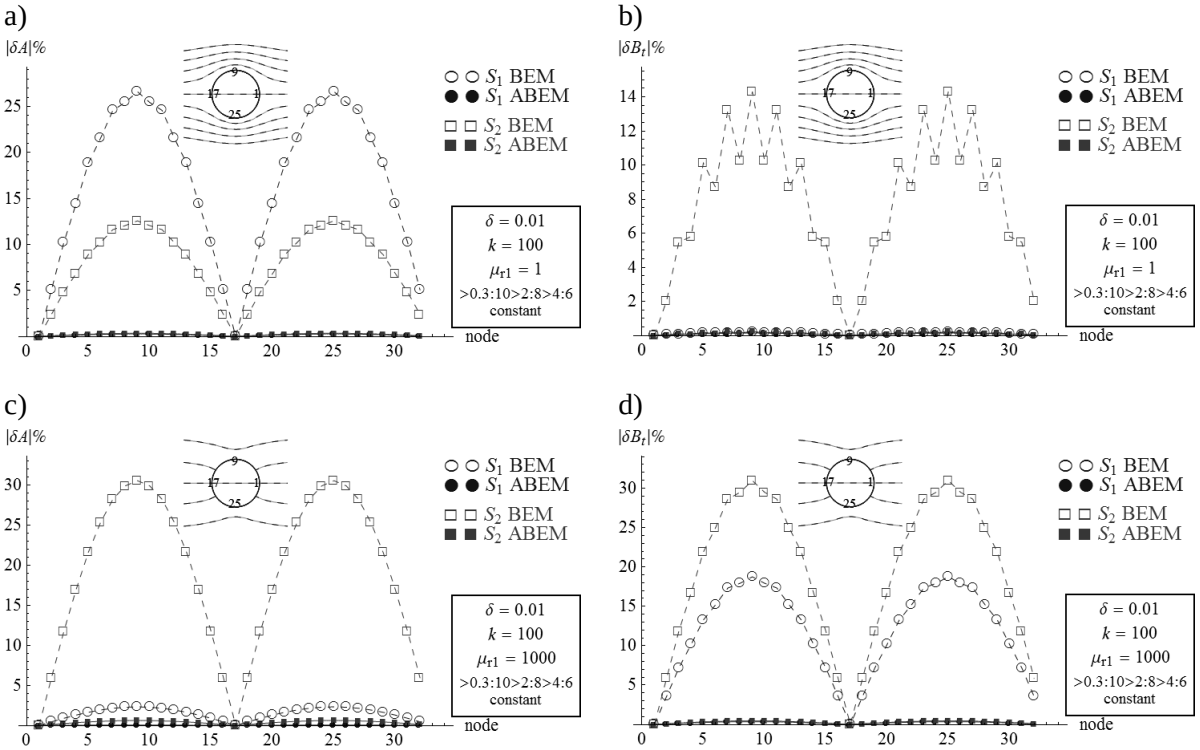

Fig. 6. Magnitudes of errors $\delta\underline{A}$ (a, c) and $\delta\underline{B}_t$ (b, d) on boundaries S_1 and S_2 for $\delta = 0.01$, $k = 100$ with $\mu_{r1} = 1$ (a, b) or $\mu_{r1} = 1000$ (c, d) for 32 constant elements

Rys. 6. Magnitudy błędów $\delta\underline{A}$ (a, c) i $\delta\underline{B}_t$ (b, d) na brzegach S_1 i S_2 dla $\delta = 0.01$, $k = 100$ oraz $\mu_{r1} = 1$ (a, b) i $\mu_{r1} = 1000$ (c, d) dla 32 elementów stałych

Figure 7 concerns a thin (δ = 0.01) magnetic shield (μ_{r1} = 1000) with $\underline{k}$ = 0, what corresponds to a static magnetic field (ω = 0), or non-conductive shield (γ_1 = 0). Both models give results of comparable errors. Since $\delta/\mu_{r1} = 10^{-5} << 1$, the approximate model works well also in this case.

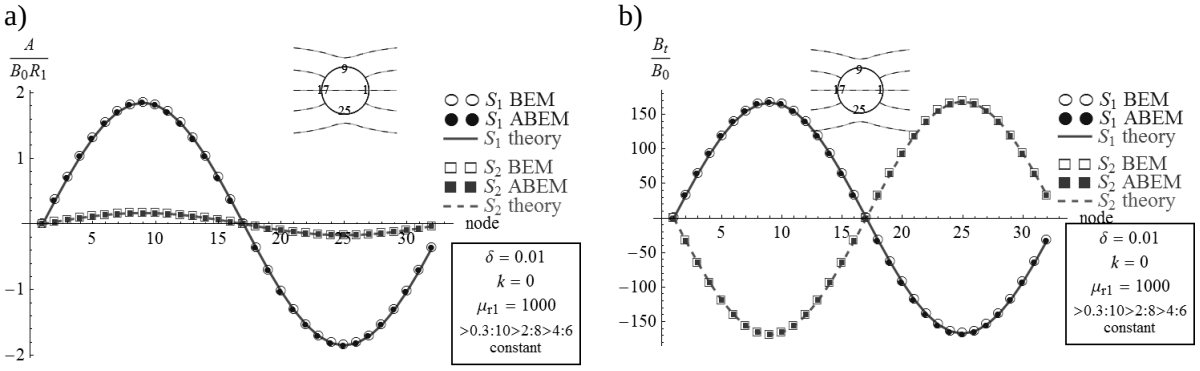

Fig. 7. Values of potential A (a) and tangential component of magnetic flux density B_t (b) on boundaries S_1 and S_2 for δ = 0.01, $\underline{k}$ = 0, μ_{r1} = 1000

Rys. 7. Wartości potencjału A (a) i składowej stycznej indukcji magnetycznej B_t (b) na brzegach S_1 i S_2 dla δ = 0.01, $\underline{k}$ = 0, μ_{r1} = 1000

3.3. C-shape shell

To make sure the approximate model works good not only for shields of circular cross-section, a more complicated shape was also tested. This was a C-shape shell of internal and external radii a and 2a, respectively, and gap angle of 90°. The shape is visible in small insets in Figure 8. The relative thickness was defined as $\delta = d/a$, and the dimensionless parameter of skin effect $\underline{\kappa} = k + \mathrm{j}k = \kappa a$. Figures 8-9 show magnitudes of potential $\underline{A}$ and tangential component of magnetic flux density $\underline{B}_t$ for several sets of parameter values.

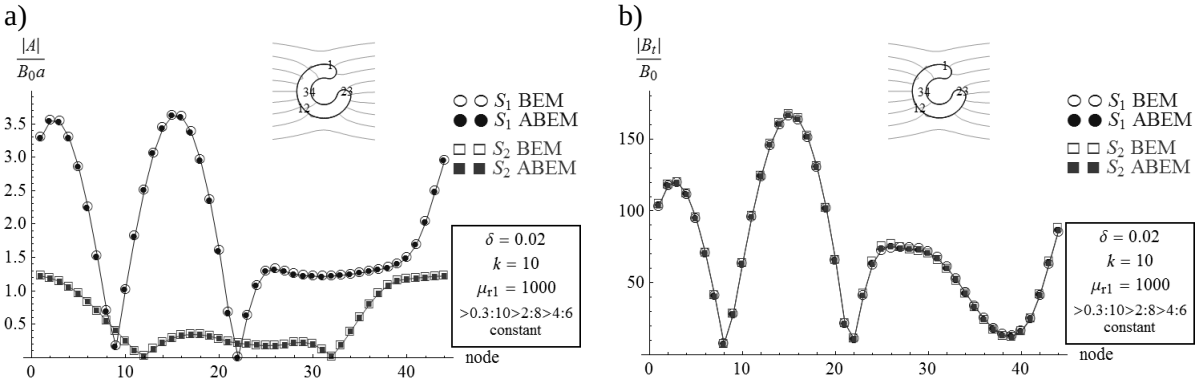

Fig. 8. Values of potential A (a) and tangential component of magnetic flux density B_t (b) on boundaries S_1 and S_2 of C-shape shell for δ = 0.02, $\underline{k}$ = 10, μ_{r1} = 1000

Rys. 8. Wartości potencjału A (a) i składowej stycznej indukcji magnetycznej B_t (b) na brzegach S_1 i S_2 powłoki C-kształtnej dla δ = 0.02, $\underline{k}$ = 10, μ_{r1} = 1000

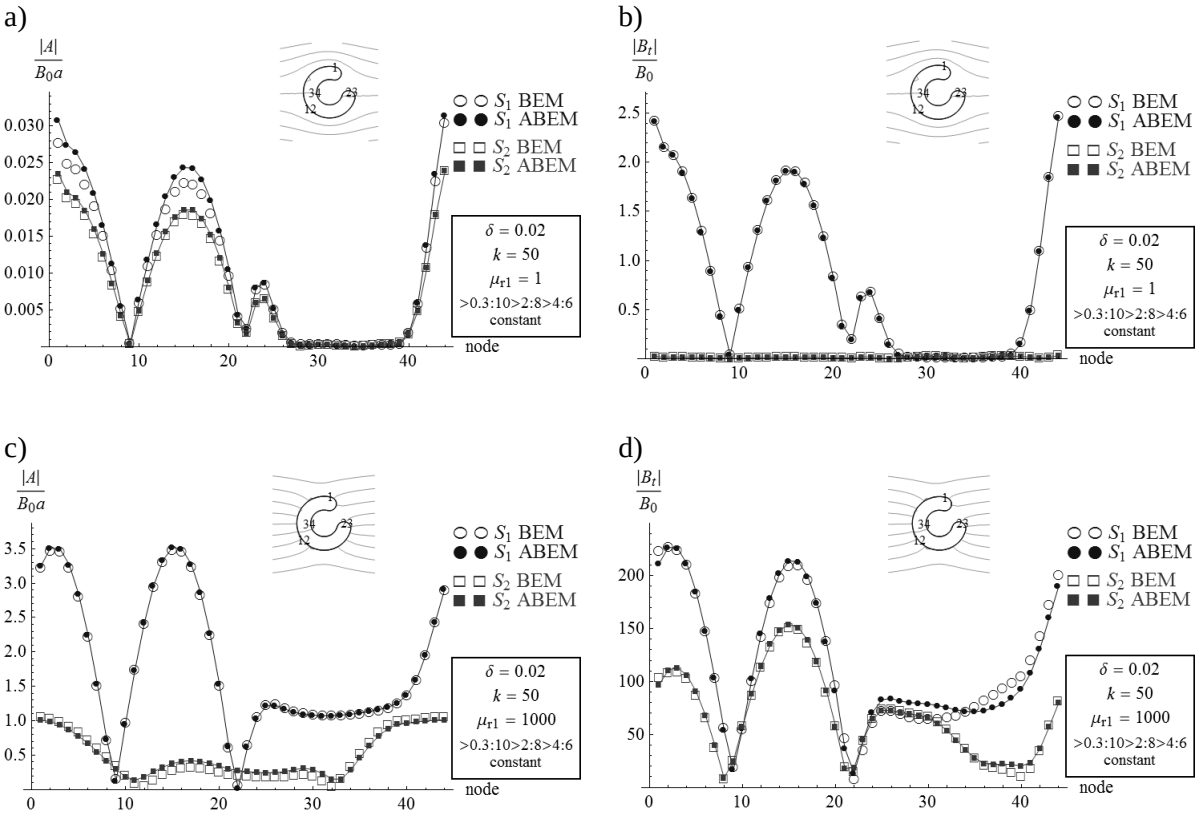

Fig. 9. Magnitudes of potential $\underline{A}$ (a, c) and tangential component of magnetic flux density $\underline{B}_t$ (b, d) on boundaries S_1 and S_2 of C-shape shell for $\delta = 0.02$, $k = 50$ with $\mu_{r1} = 1$ (a, b) or $\mu_{r1} = 1000$ (c, d)

Rys. 9. Magnitudy potencjału $\underline{A}$ (a, c) i składowej stycznej indukcji magnetycznej $\underline{B}_t$ (b, d) na brzegach S_1 i S_2 powłoki C-kształtnej dla $\delta = 0.02$, $k = 50$ oraz $\mu_{r1} = 1$ (a, b) i $\mu_{r1} = 1000$ (b, d)

Both models give similar results, although there are small differences (Figures 9a and d). To find out which model is more accurate, additional tests involving comparisons with results given by other methods are required. However, the differences are not large, so that even if the approximate model is less accurate in these cases, its evident advantages (smaller system of equations, no nearly singular integrals) should partially compensate its possible lacks.

4. CONCLUSIONS

The approximate BEM model, which combines BEM and semi-analytical solution, was proposed as a method of analyzing the time-harmonic magnetic field nearby thin closed shells, like long electromagnetic shields of constant cross-section, e.g. cylindrical. Small thickness of such shells can be a serious problem in numerical computations. The standard BEM model works well for sufficiently thick shells. For thinner shells it requires very accurate evaluating of nearly singular integrals. Numerical tests showed that this can be unreachable even with use of very sophisticated methods of numerical integration, like those which have been built in the Mathematica. As a result, it can give considerable errors if the

thickness of the shell is too small. On the other hand, the approximate BEM model works the better the smaller δ, and no nearly singular integrals need evaluation. Both theoretical analysis of cylindrical shell of circular cross-section and numerical tests for various shaped shells show that the approximate BEM model works well for large values of $|\kappa|$, and also for smaller $|\kappa|$ with additional requirement that δ/μ_{r1} should be sufficiently small. The conditions are usually fulfilled in possible practical applications. It is interesting that constant elements usually give smaller numerical errors than quadratic do (with the same set of field approximation nodes and the same order of Gaussian quadratures).

The key advantages of the approximate BEM in comparison with the standard BEM, are:

- smaller equation system,
- no nearly singular integrals (for sufficiently regular boundary),
- no need to evaluate BEM integrals with fundamental solution (10),
- good for very thin shells.

The main disadvantage is that it uses an approximate solution for the layer, which cannot be proved to be correct for all cases. Despite this, the approximate model is worth taking into account. Its usability in the considered class of problems was confirmed. Further research should focus on:

- introducing varying thickness,
- developing the model for open shells.

BIBLIOGRAPHY

1. Bolkowski S., Stabrowski M., Skoczylas J., Sroka J., Sikora J., Wincenciak S.: Komputerowe metody analizy pola elektromagnetycznego. WNT, Warszawa 1993.
2. Brebbia C.A.: The boundary element method for engineers. Pentech Press, London 1978.
3. Jabłoński P.: Approximate BEM analysis of thin conductive shell in static electroconductive field. Kwartalnik "Elektryka" 2011 z. 4 p. 41-54.
4. Jabłoński P.: Approximate BEM analysis of thin electromagnetic shield. Proceedings of XXXIV IC-SPETO 2011, Gliwice-Ustroń 18-21.05.2011, s. 17-18.
5. Jabłoński P.: Elimination of thin magnetic shell in magnetic screen analysis by means of BEM. Proceedings of XV Conference Computer Applications in Electrical Engineering, Poznań, 19-21.04.2010, s. 39-40.
6. Jabłoński P.: Metoda elementów brzegowych w analizie pola elektromagnetycznego. Wyd. Pol. Częstochowskiej, Częstochowa 2004.
7. Kirshnasamy G., Rizzo F.J.: Boundary integral equations for thin bodies. "International Journal for Numerical Methods in Engineering" 1994, Vol. 37, p. 107-121.

8. Krähenbühl L., Muller D.: Thin layers in electrical engineering. Example of shell models in analyzing eddy-currents by boundary and finite element methods. "IEEE Transactions on Magnetics" 1993, Vol. 29, No. 3, p. 1450-1455.
9. Król K., Sawicki D., Sikora J.: Zmodyfikowana metoda elementów brzegowych dla cienkich warstw. „Przegląd Elektrotechniczny" 2010, No. 7(86), s. 163-165.
10. Kurgan E.: Analiza pola magnetostatycznego w środowisku niejednorodnym metodą elementów brzegowych. Rozprawy Monografie 81, Uczelniane Wyd. Nauk.-Dyd., Kraków 1999.
11. Kurgan E.: Analysis of magnetic field in thin shell structures by boundary integral method. Proc. of XXI Seminar on Fundamentals of Electrotechnics and Circuit Theory, Gliwice-Ustroń 1998, p. 171-176.
12. Piątek Z., Jabłoński P.: Podstawy teorii pola elektromagnetycznego. WNT, Warszawa 2010.
13. Sikora J.: Podstawy metody elementów brzegowych. Zagadnienia potencjalne pola elektromagnetycznego. Wyd. Książkowe Inst. El., Warszawa 2009.
14. Sikora R.: Teoria pola elektromagnetycznego. WNT, Warszawa 1997.

Recenzent: Prof. dr hab. inż. Janusz Walczak
Wpłynęło do Redakcji dnia 20 listopada 2011 r.

Dr inż. Paweł JABŁOŃSKI

Politechnika Częstochowska, Wydział Elektryczny
Instytut Elektrotechniki Przemysłowej
ul. Armii Krajowej 17; 42-200 CZĘSTOCHOWA

tel.: (34) 3250 306; e-mail: yaboo@el.pcz.czest.pl